Elucidation of the Effect of Fast Pyrolysis and Hydrothermal Liquefaction on the Physico-chemical Properties of Bio-oil from Southern Yellow Pine Biomass as a Chemical Feedstock

Osei A. Asafu-Adjaye,[a,*] Yusuf Celikbag,[a] Jason Street,[b] Maria S. Peresin,[a] Maria L. Auad,[c] Sushil Adhikari,[d] and Brian Via [a,*]

Bio-oils obtained from southern yellow pine biomass from two thermochemical conversion processes, fast pyrolysis (FP) and hydrothermal liquefaction (HTL), were investigated. The effects of FP and HTL on the physical and chemical properties of the bio-oils were characterized. The HTL and FP bio-oil yields were 67 and 36 wt%, respectively. The results indicated that the physical properties of the HTL bio-oil and FP bio-oil were similar; however, there were variations in the composition of the bio-oils from the same biomass. The pH values of the FP and HTL bio-oils were 2.3 and 2.8, respectively. From the GC-MS (gas chromatography–mass spectrometry) analysis, esterified chemical compounds were prevalent in the HTL bio-oil, while phenols and phenolic derivatives were found in both bio-oils. The ^{31}P-NMR (phosphorous nuclear magnetic resonance) analysis of the bio-oils further revealed that both FP and HTL bio-oils are rich in phenolic OH and aliphatic OH functionalities, which could serve as a potential bio-polyol.

DOI: 10.15376/biores.17.2.2176-2192

Keywords: Fast pyrolysis; Hydrothermal liquefaction; Bio-oil; Southern yellow pine; Biomass

*Contact information: a: Forest Products Development Center, School of Forestry and Wildlife Sciences, Auburn University, Auburn, AL 36849 USA; b: Department of Sustainable Bioproducts, Mississippi State University, Starkville, MS 39762 USA; c: Department of Chemical Engineering. Auburn University, Auburn, AL 36849 USA; d: Department of Biosystem Engineering. Auburn University, Auburn, AL 36849 USA; *Corresponding authors: oaa0014@auburn.edu; brianvia@auburn.edu*

INTRODUCTION

Recent environmental impacts and concerns from fossil derived energy and chemicals have heightened the interest in environmental-friendly alternatives. Paramount among the renewable natural alternatives is lignocellulosic biomass, which has been shown to be a potential substitute for these fossil fuel derived products (Mathanker *et al.* 2020). This is because lignocellulosic biomass is abundant, relatively cheap, CO_2 neutral, renewable, and ecologically robust to withstand sustainable utilization. According to the US Department of Energy (DOE), 368 million dry tons of lignocellulosic biomass could sustainably be fetched from US forestlands annually (Perlack *et al.* 2005). To maximize the potential use of lignocellulosic biomass as a fuel and chemical feedstock, different techniques have been researched, namely thermochemical conversion (*e.g.*, direct, combustion, pyrolysis, gasification, and liquefaction) and bioprocesses (*e.g.*, fermentation and enzymatic reaction) (Bridgwater and Peacocke 2000; Ni *et al.* 2006). The thermochemical process is generally considered efficient in terms of processing time

relative to the bioprocesses. Thermochemical processes only require a residence time in the order of a few seconds or minutes for conversion to take place, while bioprocessing can take days or even weeks (Bridgwater 2010).

Fast pyrolysis (FP) and hydrothermal liquefaction (HTL) are thermochemical processes that are considered as essential viable routes to bio-based chemicals and liquid fuels. The FP process relies on the thermal decomposition of the polymers in biomass in the absence of oxygen. A relatively high temperature (450 to 500 °C) at atmospheric pressure with a short residence time (~1 to 2 s) is employed. The FP technique is considered as a simple process that is relatively easy to scale up, requiring low capital and investment cost (Jo *et al.* 2018). However, the drying of feedstock before pyrolysis is essential and often can be an impediment for processing. On the other hand, HTL is conducted at a relatively high pressure (5 to 20 MPa) with temperatures ranging from approximately 250 to 400 °C and a residence time of approximately 12 to 60 min. Unlike FP, HTL utilizes water as solvent in its operation, thus obviating the need for drying, and thereby accommodating wet biomass. Detailed reviews regarding FP and HTL processes could be found in literature (Peterson *et al.* 2008; Jahirul *et al.* 2012; Tekin *et al.* 2014; Gollakota *et al*. 2018).

Fast pyrolysis and HTL processes produce gases, solids (char), and liquids (bio-oil). The distribution and composition of bio-oil, char, and gaseous fractions formed depend mostly on the feedstock and processing parameters such as pre-treatment, temperature, heating rate, carrier gas, pressure, post-treatments, *etc*. (Hu *et al.* 2019). The applications and utilizations of char and gaseous products of FP and HTL can be found elsewhere (Borsodi *et al.* 2016; Goswami *et al.* 2020). The scope of this study covered bio-oil only. Bio-oil refers to the liquid product of pyrolysis and thermochemical liquefaction of biomass. Bio-oil is considered a thermochemical product that rivals petroleum crude oil. Detailed applications of bio-oil are discussed in previous literature (Hu and Gholizadeh 2020).

The physical and chemical properties of the bio-oil may vary, depending on the processing conditions. To compare the effect of FP and HTL on the composition of bio-oil, the same feedstock should be used in the process. Studies on the characterization of bio-oil produced by HTL and FP using the same biomass are limited. The available studies have focused on algae (Jena and Das 2011; Vardon *et al*. 2012; Hognon *et al.* 2015; Chiaramonti *et al.* 2017; Jayaseelan *et al.* 2020). Two of such studies on lignocellulosic biomass are on beech wood, a hardwood (Heidari *et al.* 2014; Haarlemmer *et al.* 2016). In this study, the physical and chemical properties of bio-oils from southern yellow pine as influenced by FP and HTL (using water/ethanol as solvent) were characterized. This study is the first work employing ^{31}P-NMR (phosphorous nuclear magnetic resonance) in quantifying and elucidating the distribution of hydroxyl (OH) moieties in bio-oil obtained from pyrolysis and HTL from the same biomass. Characterization of the OH functionalities could be used to track bio-oil aging and aids in efficient utilization of bio-oil as a bio-polyol.

EXPERIMENTAL

Materials

Southern yellow pine planer shavings were used as the feedstock for both the FP and the HTL processes in this study. The feedstock was sourced from Southeastern Timber

Products in Ackerman, MS, USA. Southern yellow pine planer shavings were air dried to 8 to 10% moisture content. In a hammer mill (New Holland grinder model 358, New Holland, PA), the planer shavings were ground, and the sawdust was sieved with a sieve shaker, and the pine particles retained between 0.3 and 0.5 mm were used for both FP and HTL bio-oil production. Chemicals used in this study were purchased from VWR (Philadelphia, USA) as reagent grade. However, the 2-chloro-4,4,5,5-tetramethyl-1,3,2-dioxaphospholane (TMDP) and phosphorylating agent for ^{31}P-NMR analysis were purchased from Sigma Aldrich (Burlington, USA). The chemicals were used as received from vendors.

Methods

Hydrothermal liquefaction process

Southern yellow pine liquefaction using the HTL process was carried out in a 1 L Parr reactor furnished with a stirrer (Model 4577 HP/HT pressure reactor, Parr Instrument Company, Moline, IL, USA) and controller. In a typical run, the reactor was charged with 50 g of southern yellow pine saw dust and 500 g of solvent (1/10: Biomass/solvent). The solvent comprised of water/ethanol mixture (1/1, wt/wt). After sealing the reactor, nitrogen gas was introduced into the reactor to displace the remaining air. The reactor was pressurized with nitrogen gas to 2 MPa and heated up to 300 °C with constant stirring. The reaction temperature was kept constant for 30 min after the set temperature was reached. The reactor was submerged in a water/ice bath to terminate the liquefaction reaction process after 30 mins. Bio-oil was obtained after filtration of the slurry followed by solvent extraction using dichloromethane and solvent removal by rotary evaporation. The selected HTL conditions followed the optimized bio-oil yield for bio-polyol production done in the authors' lab (Celikbag *et al.* 2016). A schematic diagram of the Parr reactor is shown in (Fig. 1a). The bio-oil yield was calculated as follows:

$$Yield_{\ bio-oil}\ (wt\%) = \frac{Weight_{\ bio-oil}}{Weight_{\ biomass}} \times 100 \quad (1)$$

Fast pyrolysis (FP) process

Fast pyrolysis bio-oil was made from the same southern pine wood particles but further dried to 6 to 7% moisture content using a similar manner mentioned in a previous study (Li *et al.* 2013) without any spraying of chemicals or water to cool the vapors. Fast pyrolysis of untreated southern pine was conducted in a 7 kg h^{-1} auger-fed pyrolysis reactor (Mississippi State University (MSU)) in triplicate, and the product yields were averaged. Nitrogen gas was used to exclude oxygen from the system at the feed hopper. Pyrolysis reactions occurred in a reactor pipe 76.2 mm in diameter and 1143 mm long. The auger speed was 10 rpm at the applied pyrolysis temperature of 450 °C with a gas residence time of approximately 2 s. The heat for the pyrolysis reactions was provided by multiple heaters along the reactor pipe, including a preheating zone (300 °C), a pyrolysis zone (450 °C), and a post-reaction zone (300 °C). A schematic of the reactor can be seen in (Fig. 1b).

Distillation

The bio-oil produced from each condenser was mixed and referred to as whole bio-oil. There was a separate collection from another run where bio-oil was collected from condenser 3; this was referred to as "aqueous bio-oil". The same lighter components were distilled from both the whole and aqueous bio-oil types at a range of 35 to 99 °C. Distillation of the bio-oil was performed using the same equipment discussed in Street *et*

al. (2016). The packed column distillation apparatus used in this study was a BR 9600 packed column distillation system.

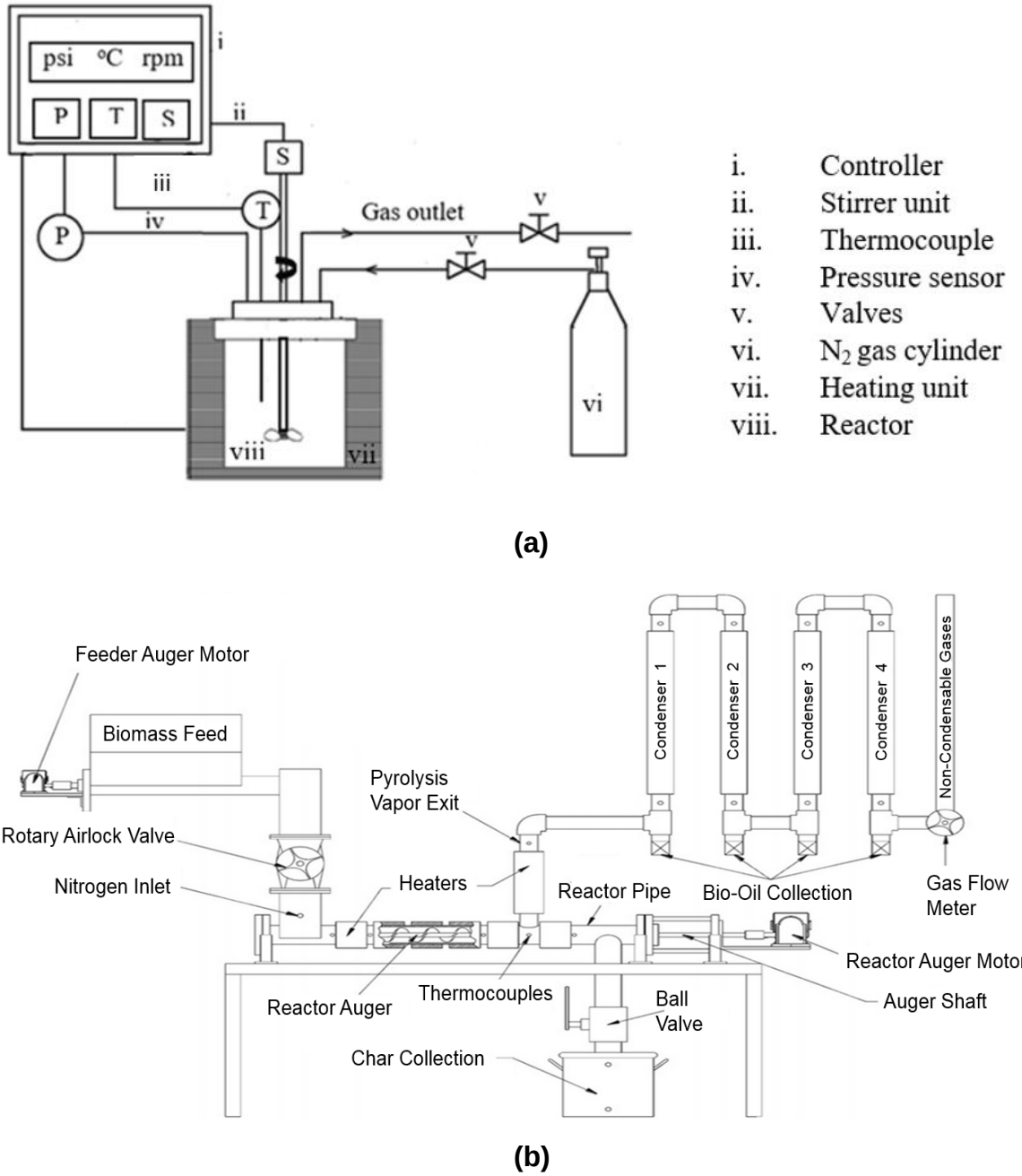

Fig. 1. (a) Schematic reactor used for the hydrothermal liquefaction; (b) schematic of the auger pyrolysis reactor at MSU used for the bio-oil production

The distillation system was obtained from BR Instruments (Easton, MD, USA). The bio-oil to be distilled was placed in a 3L round bottom flask which contained a magnetic stirrer. The flask was placed in a heating mantle and secured to the column. Two thermocouples were placed and secured in the system. One thermocouple was in a glass thermowell in a round-bottom flask to measure the temperature of the fluid in the flask,

and the second thermocouple was placed on top of the packed bed distillation column to measure the temperature of the vapors leaving the column to be further cooled by the condenser. Four calibrated receivers were placed and secured in the system after the condenser to collect the desired fractions. The distillation was automatically controlled with the BR M690 PC-interface (BR Instruments, Easton, MD, USA). A heating rate (30% of full power of the heater) was defined in the software to bring the fluid to the initial boiling point. The reflux ratio of 5:1 was controlled with an automatic solenoid valve and was controlled by the software. The temperature of each cut (temperature to change receivers), and final fluid temperature (temperature in the flask) were also controlled and recorded by the software. The distillation column was left to stabilize for approximately 1 h after the bio-oil started boiling (until the pot and vapor temperature remained stable). The distillation process was ceased when the boiling pot reached 120 °C to keep the longer chained hydrocarbons from cracking and to lessen the possibility of instantaneous polymerization of the components.

Physical properties analysis of the HTL and FP bio-oils

Physical properties comprising viscosity, elemental analysis, heating value, density, water content, ash content, and pH analysis of the biomass and both HTL and FP bio-oils were characterized. The dynamic viscosity of the bio-oils was determined using Bohlin rheometer (model CV100; Malvern Panalytical, Westborough, MA, USA) at 25, 40, and 60 °C. Truncated cone and plate geometry with shear rates from 0.5 to 150 s^{-1} and a plate gap of 1000 μm was utilized in the viscosity analysis of the bio-oils. The pH of the HTL, and FP bio-oils were measured using a pH meter (model PC 510, Oakton Instruments, Oakton, IL, USA). Proximate analysis was performed in duplicate following ash content analysis (ASTM E1755-01, 2020), moisture analysis (ASTM E871-82, 2019), volatile matter (ASTM E872-82, 2019), and fixed carbon by difference. A volumetric Karl Fischer titrator (model V20; Mettler Toledo, Columbus, OH, USA) using a hydranal-composite 5 solution (Sigma-Aldrich) was used to measure the water content of the bio-oils. The density of the bio-oils was determined using a 2 mL, calibrated density bottle filled with a known mass of bio-oil. The ultimate analysis to determine the elemental composition of the bio-oils was performed in duplicate using a CHNS/O analyzer (model CHNS/O 2400, PerkinElmer, Waltham, MA, USA). The oxygen content was calculated by difference. An oxygen calorimeter (model C2000; IKA-Werke, Staufen, Germany) was used to determine the higher heating value (HHV) of the bio-oils.

Gas chromatography–mass spectrometry (GC-MS) analysis of HTL and FP bio-oils

Chemical constituents of the HTL and FP bio-oils were conducted using an Agilent 7890 GC/5975 MS equipped with a DB-1701 column (30 mm, 0.25 mm inner diameter, and 0.25 mm film thickness). Approximately 150 mg of FP bio-oil was mixed with 3 mL of methanol, and it was diluted to 10 mL with dichloromethane. The HTL bio-oil followed similar procedure except that the dichloromethane was mixed first. The diluted samples were injected into the column respectively. The column initial temperature (40 °C) was maintained for 2 min and then increased to 250 °C at 5 °C/min. The final temperature was held for 8 min. Ultra high purity helium (99.999%) from Airgas, Inc. (Charlotte, NC, USA) was used as the carrier gas set at a flow rate of 1.25 mL/min. The HTL and FP bio-oils compounds were identified by comparing the mass spectra to the National Institute of Standards and Technology (NIST) mass spectral library.

Thermal gravimetric analysis (TGA)

Thermal gravimetric analysis of the FP and HTL bio-oils were performed using a TA Instruments TGA Q500 thermal gravimetric analyzer (New Castle, DE, USA). The bio-oil samples were heated under a N_2 atmosphere at 20 mL/min from ambient to 800 °C at heating rate of 10 °C/min.

Hydroxyl (OH) group analysis by ^{31}P-NMR

Hydroxyl group analysis of the bio-oils (HTL and FP) were conducted using ^{31}P-NMR. The phosphitylation method employed followed methodology from (Celikbag *et al*. 2015). The ^{31}P-NMR spectra were obtained with a Bruker Avance II 250 MHz spectrometer (Bruker, Billerica, MA, USA) using inverse gated decoupling pulse sequence with a 90° pulse angle, 25 s pulse delay, and 128 scans following the methods of Ben and Ragauskas (2011). Two replicates of each bio-oil were made.

Fourier transform infrared (FTIR) analysis

Attenuated total reflection Fourier transform infrared (ATR-FTIR) spectra of HTL, and FP bio-oils, were respectively acquired between 4000 and 650 cm^{-1} with 4.00 cm^{-1} resolution and 32 scans using an ATR-FTIR spectrometer (Model Spectrum400, PerkinElmer, Waltham, MA) to determine the functional groups. All ATR-FTIR spectra were collected at room temperature.

RESULTS AND DISCUSSION

Biomass Characterization

The inherent composition, elemental and proximate analyses of southern yellow pine biomass used for the FP and HTL techniques are presented in Table 1. The composition, ultimate analysis, and proximate analysis of the feedstock were consistent with other reported pine biomass species (Mahadevan *et al.* 2015; Chiodo *et al.* 2016). Higher volatile matter coupled with low ash content are desirable features for feedstock in thermal conversion because alkali metals in ash may serve as a catalyst to change the pyrolysis depolymerization mechanism and cause slag formation to occur on the walls of operational equipment (Fahmi *et al.* 2007). Ash content was not studied in this work.

Table 1. Biomass Proximate, Ultimate, and Heating Value Analyses (Dry Basis)

Ultimate Analysis	Results (wt.%)	Proximate Analysis	Result (wt.%)
C	45.1 ± 0.1	Ash content	0.55 ± 0.01
H	6.3 ± 0.1	Volatile matter	79.14 ± 0.91
*O	48.1 ± 0.2	Moisture content	6.88 ± 0.01
N	0.3 ± 0.0	Fixed carbon	13.43 ± 0.90
S	0.2 ± 0.0	Heating value (MJ/Kg)	19.60 ± 0.02
*O is by difference; wt.% = weight percent			

Table 2. Product Yields of *Pinus spp.* by Fast Pyrolysis (FP) and Hydrothermal Liquefaction (HTL)

Yield	Fast Pyrolysis (wt.%)	Hydrothermal Liquefaction (wt.%)
Bio-oil	36 ± 3	67 ± 2
Light oil (aqueous phase)	18 ± 1	14 ± 2
Gas	19 ± 2	16 ± 3
Char	27 ± 1	3 ± 1
wt.% = weight percent		

Fast pyrolysis and hydrothermal liquefaction product yield and characteristics

Fast pyrolysis and HTL bio-oils are viscous, and dark brownish in color. However, FP bio-oil has a characteristic strong smoky scent, while HTL bio-oil (with water/ethanol as co-solvent) has a pungent sweet-smoky, vanilla-like odor. Fast pyrolysis product yields were estimated as the weight percentage of individual product phase (bio-oil, light oil, and char) relative to the weight of the dried feedstock. Gas yield was calculated by difference (100 - (bio-oil, light oil, and char) wt%. The product yields were influenced by the thermochemical conversion process (*i.e.*, FP and HTL) given the same feedstock (Table 2). Comparatively, the HTL process had approximately twice as much bio-oil yield (67%) as the FP process (36%). Apart from the process conditions, the high bio-oil yield observed in the HTL could be attributed to the addition of ethanol in the HTL process. Previous work demonstrated a greater synergy between water/ethanol in increasing bio-oil yield compared to water only in HTL process. The bio-oil yield using water/ethanol as solvent was about three times higher than using water only (Celikbag *et al.* 2016). Biswas *et al.* (2020) found almost a 10-fold increase in bio-oil yield with water/ethanol as solvent compared to water only. Additionally, the reduced amount of char formation was closely associated with improved bio-oil yield with the addition of ethanol to water (Liu *et al.* 2013). A hydrogen donor solvent such as ethanol could reduce the formation of char by stabilizing reactive free radicals generated from the fragmentation of feedstock during the HTL process from repolymerization (Yuan *et al.* 2007). It is also known that ethanol/water at subcritical water conditions enhances the solubility of high molecular weight compounds and dissolvability of oily products (Liu *et al.* 2013). Thus, it could be inferred that the lack of hydrogen donor solvent in the FP process could have promoted char formation and reduced bio-oil yield. FP and HTL of beech wood revealed a similar pattern of improved bio-oil yield and reduced char yield in the HTL process with NaOH acting as a catalyst. The FP bio-oil yield was lower than the HTL (Haarlemmer *et al.* 2016). Another study comparing pyrolysis and HTL of *Chlamydomonas reinhardtii*, a green microalgae, suggested generally that HTL bio-oil yield was higher than pyrolysis bio-oil yield (Hognon *et al*. 2015). Analysis of slow pyrolysis and the HTL of defatted algal biomass study also confirmed lower pyrolysis bio-oil and high solid (char) yields than the HTL (Vardon *et. al.* 2012).

Bulk properties of fast pyrolysis and hydrothermal liquefaction bio-oil

The high oxygen content (Table 3) may have resulted from functional groups such as alcohols, carboxylic acids, and phenols during the thermochemical conversion process. Nonetheless, these oxygenated compounds may be essential in bio-based polymer synthesis.

Table 3. Ultimate Analysis and Physical Properties of FP Bio-oil and HTL Bio-oil (Dry Basis)

Ultimate Analysis	FP Bio-oil (wt%)	HTL Bio-oil (wt%)	Properties	FP Bio-oil	HTL Bio-oil
C	54.5 ± 0.20	61.7 ± 0.3	MC (%)	15.5 ± 0.1	14.6 ± 0.30
O	38.7 ± 0.20	30.8 ± 0.3	pH	2.3 ± 0.0	2.8 ± 0.01
N	0.2 ± 0.01	0.2 ± 0.0	Ash (%)	0.01 ± 0.0	0.01 ± 0.0
S	0.1 ± 0.01	0.1 ± 0.0	Density (Kg/m³)	1287 ± 17	1013 ± 13
H	6.5 ± 0.10	7.2 ± 0.10	Heating Value (MJ/Kg)	23.3 ± 0.1	28.9 ± 0.16
Oxygen content estimated by difference; MC = moisture content					

For example, OH groups in bio-oil are considered the primary active functional groups giving bio-oil polyol attributes (Sasaki *et al*. 2013). The respective pH values of FP and HTL bio-oils indicate that both bio-oils are acidic; this is a disadvantage as a fuel but the product may serve as a catalyst in adhesive synthesis (Barde *et al*. 2019).

Viscosity analysis

Viscosity analysis was carried out at 25, 40, and 60 °C for FP and HTL bio-oil with varying shear rates from 0.1 to 150 s^{-1}, as presented in (Fig. 2). Generally, the viscosity of the bio-oils decreased with increased temperature. For example, the viscosity of FP bio-oil decreased from 0.226 Pa.s at 25 °C to 0.164 Pa.s at 60 °C. At low shear rate (shear rate < 25 s^{-1}), the viscosity was high and both the FP and HTL bio-oils behaved as a non-Newtonian fluid. A Newtonian fluid behavior was observed at a higher shear rate (shear rate > 25 s^{-1}). A previous study demonstrated that bio-oil viscosity is shear rate and temperature dependent (Thangalazhy-Gopakumar *et al*. 2010). Comparatively, for all the temperatures studied, the viscosity of the FP bio-oil was higher than the HTL bio-oil. However, the viscosity of HTL bio-oil of beech wood was much higher than fast pyrolysis bio-oil of the same feedstock (Haarlemmer *et al*. 2016). The seemingly conflicting findings could be explained by the HTL solvent or catalyst used. The water and sodium hydroxide used in the liquefaction process by Haarlemmer *et al*. (2016) may not have been efficient in preventing repolymerization of the reactive low molecular weight compounds from forming high molecular weight compounds. The presence of ethanol during the HTL process may have promoted the solubility of high molecular weight compounds and prevented re-polymerization of the bio-oil components, resulting in low viscosity.

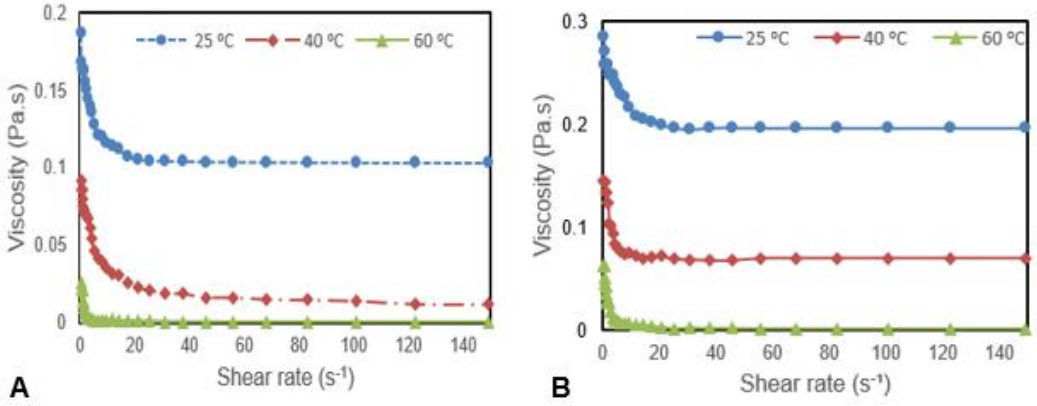

Fig. 2. Viscosity of bio-oil at selected shear rates produced by hydrothermal liquefaction (A) and fast pyrolysis (B)

Chemical characteristic of FP and HTL bio-oils

The GC-MS analysis of the FP and HTL bio-oils is shown in Fig. 3. The compounds identified were complex and were grouped into phenolics, acids, esters, ketones, aldehydes, anhydrosugars, furans, and others. Phenolic compounds (phenols and phenolic derivatives) originating from lignin degradation were dominant in the bio-oils. Of the total peak area percentage analyzed, phenolic compounds constituted ~41% and ~32% of the FP and HTL bio-oils, respectively. Phenolic compounds such as phenol, p-cresol, guaiacol, vanillin, and isoeugenol were common in both FP and HTL bio-oils. These compounds such as vanillin and eugenol serve as a feedstock for food flavoring and fragrance industries. Previous studies on bio-oils from pine revealed similar compounds (Thangalazhy-Gopakumar *et al.* 2010; Mahadevan *et al.* 2015). Acetic acid was the main carboxylic acid in the bio-oils. Carboxylic acids are known to catalyze the repolymerization of bio-oil leading to high viscosity and increased molecular weight (Jo *et al.* 2018). While the acid peak area % of FP bio-oil was relatively high (~7%), the co-solvent (water/ethanol) of the HTL bio-oil may have reduced the formation of carboxylic acid species (~2%). It seems that the addition of ethanol favored the formation of esters by condensation reaction with the carboxylic acids (Fig. 3 insert) in the HTL bio-oil. Thus, a higher ester % peak area (~25%) of HTL bio-oil compared to FP bio-oil (~ 4%). Apart from the acids, the presence of aldehyde, ketones, anhydrosugars, and furans indicated that the bio-oils contain substantial amounts of oxygenated compounds. The occurrence of these oxygenated compounds have mainly been linked to holocellulose degradation (Alén *et al.* 1996). The unidentified anhydrosugar peak in the HTL bio-oil could possibly be attributed to the efficient phase separation of the light-oil (aqueous phase) from the bio-oil in contrast to the FP bio-oil. Compounds grouped under the "other" category mainly consisted of hydrocarbons (like trans-1,4-hexadiene; ethylidenecyclobutane), nitrogenous (such as 1,3-propanediamine, N-methyl-), and sulfur (2-acetyl-3-methylthiophene; 2-hydroxyethyl vinyl sulfide) containing compounds.

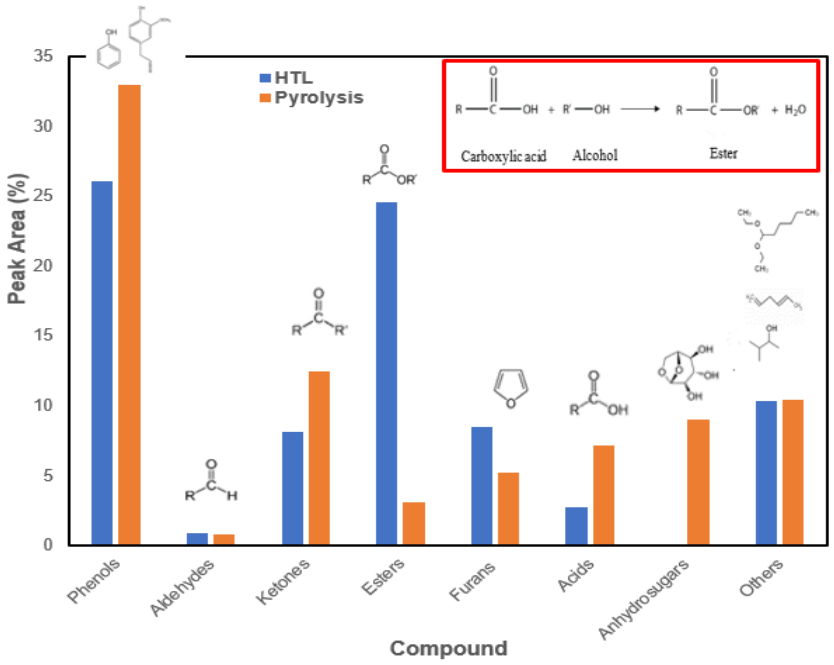

Fig. 3. Chemical composition of FP and HTL bio-oil by GC-MS

Thermogravimetric analysis

The thermal stabilities of the FP bio-oil and HTL bio-oil were measured as weight percentage loss of the bio-oils with increased temperature. Several studies have underscored the intrinsic drawbacks of GC-MS in elucidating the total chemical constituents of bio-oil. This is because the GC column vaporizes highly volatile compounds with boiling points below the column temperature, usually less than 300 °C (Nazari *et al.* 2015; Zhang *et al.* 2017). At temperatures below 300 °C, less than 20 to 50 wt% of bio-crude oils could be volatilized (Sun *et al*. 2010). The weight loss percentage curves (TG) with the corresponding derivative weight loss curves (DTG) for FP and HTL bio-oils are shown in Fig. 4. The degradation profiles of the bio-oils presented three different major stages. The initial stage was assigned to the dehydration of moisture and volatilization of low organic weight compounds such as alcohols, carboxylic acids, and aldehydes at low temperature (Zhang *et al.* 2017). This stage accounted for about 10% weight loss for the HTL bio-oil and 6% weight loss for the FP-bio-oil occurring at room temperature to 100 °C and 102 °C respectively. The maximum weight loss occurred in the second stage. At this phase, the weight loss of the FP bio-oil was about 58% at a temperature range between 100 °C and 350 °C, and 60% weight loss at a temperature range of 102 °C to 470 °C for HTL bio-oil. This stage was attributed to the cracking of phenolic compounds, vanillin, and other oligomer compounds formed due to the polymerization of the bio-oils. Weight loss at the third stage was 11% for HTL bio-oil within a temperature range of 470 to 800 °C and 22% weight loss for FP bio-oil at a temperature range of 350 to 800 °C. The third stage weight loss was imputed to chemical bonds cleavage of the heavy components of the bio-oil (predominantly lignin derivatives) as the decomposition temperature increased. The high percent weight loss for FP bio-oil at the third stage suggested that the FP process of producing bio-oil comparatively yields more macromolecule aromatic compounds. The observed difference in degradation regimes for the DTG curves could be ascribed to the different chemical species present in the bio-oil. The varying degradation temperatures for the FP and HTL bio-oils present a challenge in determining the maximum degradation temperatures for the bio-oils because the bio-oils are a complex mix of sugars and lignin derivatives, as confirmed by the FTIR and GC-MS analysis.

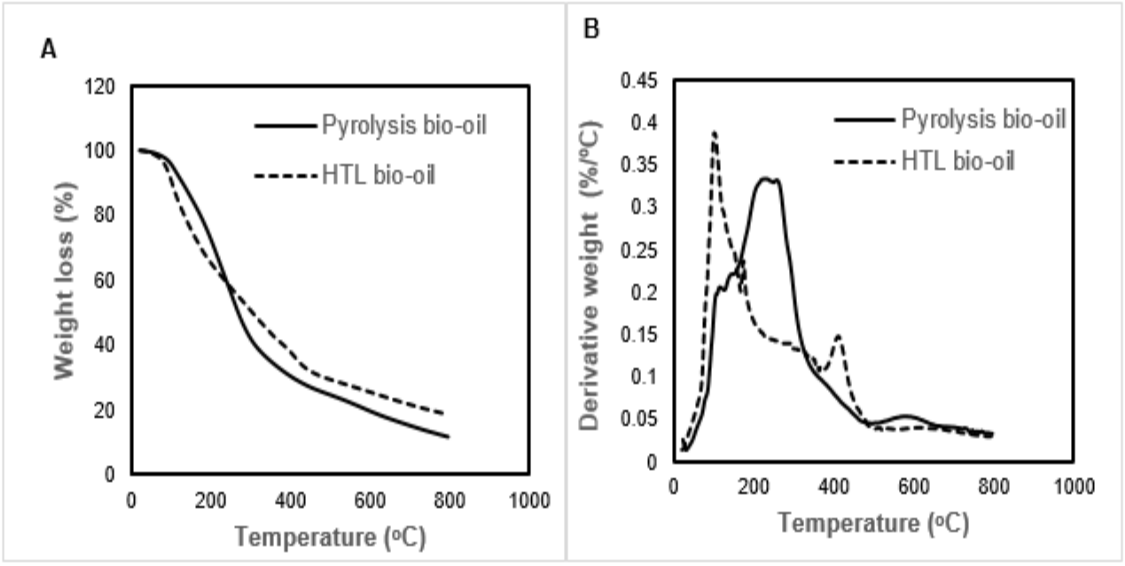

Fig. 4. TGA - A and derivative weight loss (DTG) - B curves of FP and HTL bio-oils

FTIR analysis

Functional groups characterization of the FP and HTL bio-oil is shown in the FTIR spectra in Fig. 5. It is fascinating to observe similar spectral characteristics from both FP and HTL bio-oils. The broad peak between 3100 and 3650 cm^{-1} indicated the presence of OH moieties resulting from aliphatic, acidic, phenolic, water, and aromatic OH groups in the bio-oils. The C–H stretching vibrations between 2800 and 3000 cm^{-1} and the C–H bending vibrations between 1380 and 1450 cm^{-1} suggested the presence of alkanes. The characteristic C=O peak at ~1712 cm^{-1} indicated carbonyl groups, suggesting the presence of ketones, aldehydes, and carboxylic acids in the bio-oils. The narrow absorbance peak at 1513 cm^{-1} C=C showed aromatic ring stretching vibration of alkenes due to lignin degradation products (Singh *et al.* 2015). The absorbance peak located between 1300 and 1207 cm^{-1} revealed C-O stretching, and symmetrical C-O stretching at absorbance peak ~1046 cm^{-1} suggested the possible presence of acids, phenols, or alcohols in the bio-oil (Nazari *et al.* 2015). The presence of aromatic esters was evidenced by C=O stretching in addition to the occurrence of the aromatic ring vibration between 900 and 650 cm^{-1} (Qian *et al.* 2007). The HTL and pyrolysis spectra absorbance between 878 and 650 cm^{-1} showed a likely presence of aromatic moieties (C-H in plane). Nonetheless, weak peak intensities were comparatively observed in the pyrolysis spectra at this region.

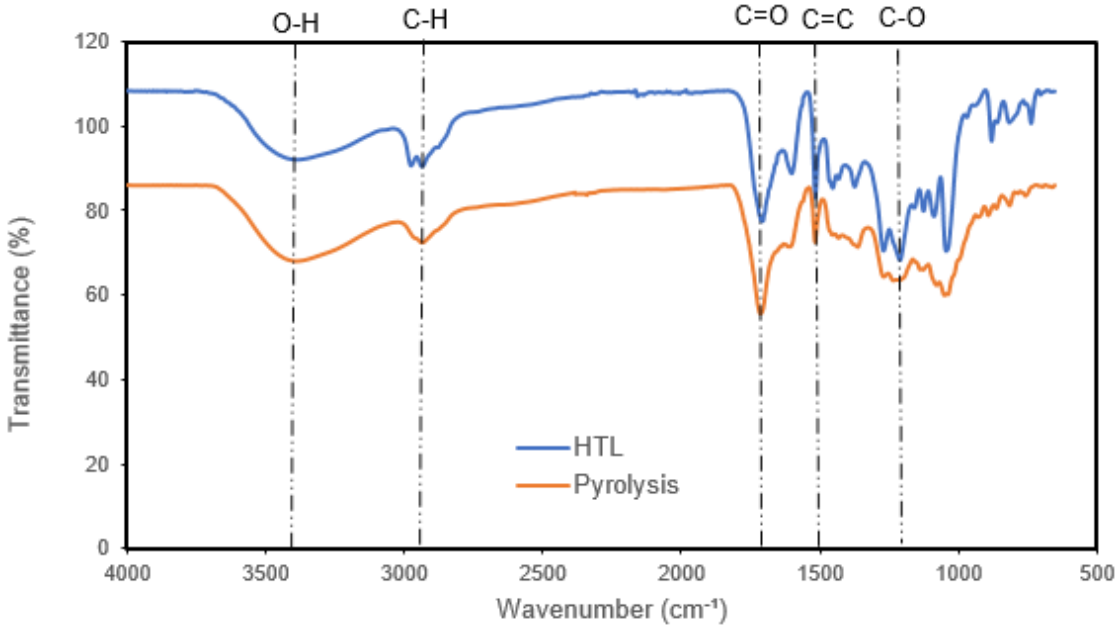

Fig. 5. FTIR spectra of fast pyrolysis and hydrothermal liquefaction derived-bio-oils

Hydroxyl (OH) group analysis of HTL and FP bio-oils by ^{31}P-NMR

The use of ^{31}P-NMR in characterizing the hydroxyl numbers of biomass lignin and biofuel precursor have been detailed by Pu *et al.* (2011). The ^{31}P-NMR method carries exceptional advantage over ^{1}H-NMR and ^{13}C-NMR in elucidating the hydroxyl content. For example: (i) ^{31}P-NMR requires relatively small amounts of the sample in its preparation; (ii) quantitative analysis of the different major hydroxyl groups is achieved within a shorter time compared to ^{13}C-NMR; and (iii) unlike ^{1}H-NMR which suffers from spectral overlap, the ^{31}P nucleus has a large range of chemical shifts providing better signal resolution and separation.

Quantitative ^{31}P-NMR analysis of the hydroxyl number (OHN) and integration regions for both FP and HTL bio-oils is presented in Fig. 6. The OHN of HTL and FP bio-oils were calculated to be 9.25 mmol/g and 10.30 mmol/g respectively. Aliphatic, phenolic, and acidic hydroxyl groups were identified and quantified respectively for HTL and FP bio-oils (in parentheses) as 54% (55%), 35% (31%), and 11% (14%) of the total OHN (supplemental Table S1). Previous studies have closely associated aliphatic OH types to the degradation of cellulose and hemicellulose, a major component of the wood (Peterson *et al*. 2008; Changi *et al*. 2015), thus, the highest OHN recorded for aliphatic OH. The p-hydroxyphenyl, monomeric phenols, catechol, and guaiacyl type of OH groups in bio-oils were attributed to the cleavage of ether bonds of lignin during FP and HTL conversion of the pine biomass (Xu *et al*. 2014). Acidic OH in the HTL and FP bio-oils were 1.04 mmol/g and 1.47 mmol/g respectively. Acidic OH moieties may have resulted mainly from the degradation products of hemicelluloses (Qu *et al*. 2011).

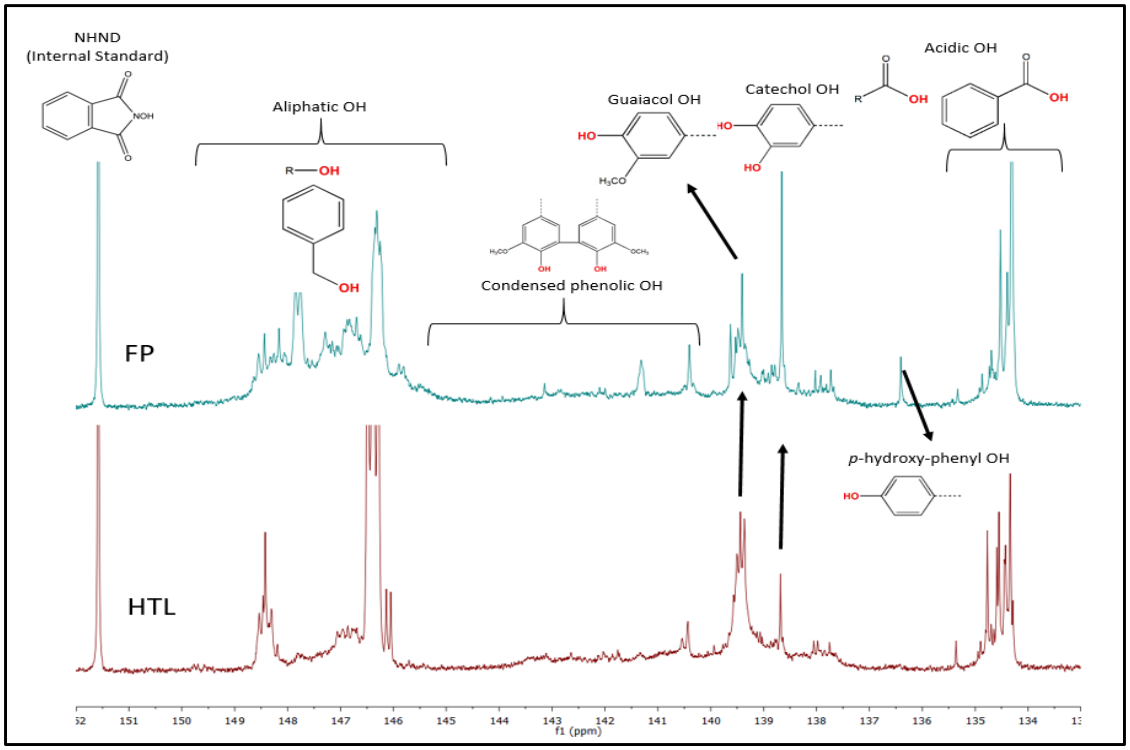

Fig. 6. ^{31}P-NMR spectra for the FP and HTL bio-oils

CONCLUSIONS

1. The effects of fast pyrolysis (FP) and hydrothermal liquefaction (HTL) processes on the bio-oil obtained from southern yellow pine was investigated. The HTL generated high bio-oil yield relative to the FP process.
2. Fast pyrolysis derived bio-oil was higher in viscosity relative to the HTL bio-oil. Similar functional groups but different thermal and chemical compositions were observed *via* thermogravimetric analysis (TGA), Fourier transform infrared (FTIR), and gas chromatography-mass spectrometry (GC-MS) analysis for the bio-oils.

3. Esterified chemical compounds characterized the HTL bio-oil. The FP bio-oil had a substantial amount of phenolic compounds, comparatively. High concentration of OH numbers were demonstrated *via* quantitative ^{31}P-nuclear magnetic resonance (NMR) spectrometry. The OHN of FP bio-oil makes it an attractive option over HTL bio-oil for bio-polyol, although bio-oil yield should be considered.

ACKNOWLEDGMENTS

This work was supported by the Agriculture and Food Research Initiative − "Hydrophobic Bio-oil-Epoxy Binders for Wood Composites" (Project Award No. 2017-67021-26134).

REFERENCES CITED

Alén, R., Kuoppala, E., and Oesch, P. (1996). "Formation of the main degradation compound groups from wood and its components during pyrolysis," *J. Anal. Appl. Pyrolysis* 36(2), 137-148. DOI: 10.1016/0165-2370 (96)00932-1

ASTM E871-82 (2019). "Standard method for moisture analysis of particulate wood fuels," ASTM International, West Conshohocken, PA, USA.

ASTM E872-82 (2019). "Standard test method for volatile matter in the analysis of particulate wood fuels," ASTM International, West Conshohocken, PA, USA.

ASTM E1755-01 (2020). "Standard test method for ash in biomass," ASTM International, West Conshohocken, PA, USA.

Barde, M., Celikbag, Y., Via, B., Adhikari, S., and Auad, M. L. (2019). "Semi-interpenetrating novolac-epoxy thermoset polymer networks derived from plant biomass," *J. Renew. Mater.* 6(7), 724-736. DOI: 10.32604/jrm.2018.00116

Ben, H., and Ragauskas, A. J. (2011). "NMR characterization of pyrolysis oils from kraft lignin," *Energ. Fuel.* 25(5), 2322-2332. DOI: 10.1021/ef2001162

Biswas, B., Kumar, A., Fernandes, A. C., Saini, K., Negi, S., Muraleedharan, U. D., and Bhaskar, T. (2020). "Solid base catalytic hydrothermal liquefaction of macroalgae: Effects of process parameter on product yield and characterization," *Bioresour. Technol.* 307, article ID 123232. DOI: 10.1016/j.biortech.2020.123232

Borsodi, N., Szentes, A., Miskolczi, N., Wu, C., and Liu, X. (2016). "Carbon nanotubes synthetized from gaseous products of waste polymer pyrolysis and their application," *J. Anal. Appl. Pyrolysis* 120, 304-313. DOI: 10.1016/j.jaap.2016.05.018

Bridgwater, A. V. (2010). "Fast pyrolysis of biomass for energy and fuels," in: *Thermochemical Conversion of Biomass to Liquid Fuels and Chemicals*, M. Crocker (ed.), Royal Society of Chemistry, London, UK, pp. 146-191. DOI: 10.1039/9781849732260-00146

Bridgwater, A. V., and Peacocke, G. V. C. (2000). "Fast pyrolysis processes for biomass," *Renew. Sustain. Energy Rev.* 4(1), 1-73. DOI: 10.1016/S1364-0321 (99)00007-6

Celikbag, Y., Robinson, T. J., Via, B. K., Adhikari, S., and Auad, M. L. (2015). "Pyrolysis oil substituted epoxy resin: Improved ratio optimization and crosslinking efficiency," *J. Appl. Polym. Sci.* 132(28), article ID 42239. DOI: 10.1002/app.42239

Celikbag, Y., Via, B. K., Adhikari, S., Buschle-Diller, G. and Auad, M. L. (2016). "The

effect of ethanol on hydroxyl and carbonyl groups in biopolyol produced by hydrothermal liquefaction of loblolly pine: ^{31}P-NMR and ^{19}F-NMR analysis," *Bioresour. Technol.* 214, 37-44. DOI: 10.1016/j.biortech.2016.04.066

Changi, S. M., Faeth, J. L., Mo, N., and Savage, P. E. (2015). "Hydrothermal reactions of biomolecules relevant for microalgae liquefaction," *Ind. Eng. Chem. Res.* 54(47), 11733-11758. DOI: 10.1021/acs.iecr.5b02771

Chiaramonti, D., Prussi, M., Buffi, M., Rizzo, A. M., and Pari, L. (2017). "Review and experimental study on pyrolysis and hydrothermal liquefaction of microalgae for biofuel production," *Appl. Energ.* 185(2), 963-972. DOI: 10.1016/j.apenergy.2015.12.001

Chiodo, V., Zafarana, G., Maisano, S., Freni, S., and Urbani, F. (2016). "Pyrolysis of different biomass: Direct comparison among *Posidonia Oceanica*, lacustrine alga and white-pine," *Fuel* 164, 220-227. DOI: 10.1016/j.fuel.2015.09.093

Fahmi, R., Bridgwater, A. V., Darvell, L. I., Jones, J. M., Yates, N., Thain, S., and Donnison, I. S. (2007). "The effect of alkali metals on combustion and pyrolysis of *Lolium* and *Festuca* grasses, switchgrass and willow," *Fuel* 86(10-11), 1560-1569. DOI: 10.1016/j.fuel.2006.11.030

Gollakota, A. R. K., Kishore, N., and Gu, S. (2018). "A review on hydrothermal liquefaction of biomass," *Renew. Sustain. Energy Rev*. 81(1), 1378-1392. DOI: 10.1016/j.rser.2017.05.178

Goswami, M., Chaturvedi, P., Sonwani, R. K., Gupta, A. D., Singhania, R. R., Giri, B. S., Rai, B. N., Singh, H., Yadav, S., and Singh, R. S. (2020). "Application of Arjuna (*Terminalia arjuna*) seed biochar in hybrid treatment system for the bioremediation of Congo red dye," *Bioresour. Technol.* 307, Article ID 123203. DOI: 10.1016/j.biortech.2020.123203

Haarlemmer, G., Guizani, C., Anouti, S., Déniel, M., Roubaud, A., and Valin, S. (2016). "Analysis and comparison of bio-oils obtained by hydrothermal liquefaction and fast pyrolysis of beech wood," *Fuel* 174, 180-188. DOI: 10.1016/j.fuel.2016.01.082

Heidari, A., Stahl, R., Younesi, H., Rashidi, A., Troeger, N., and Ghoreyshi, A. A. (2014). "Effect of process conditions on product yield and composition of fast pyrolysis of *Eucalyptus grandis* in fluidized bed reactor," *J. Ind. Eng. Chem*. 20(4), 2594-2602. DOI: 10.1016/j.jiec.2013.10.046

Hognon, C., Delrue, F., Texier, J., Grateau, M., Thiery, S., Miller, H., and Roubaud, A. (2015). "Comparison of pyrolysis and hydrothermal liquefaction of *Chlamydomonas reinhardtii*. Growth studies on the recovered hydrothermal aqueous phase," *Biomass. Bioenerg.* 73, 23-31. DOI: 10.1016/j.biombioe.2014.11.025

Hu, X., and Gholizadeh, M., (2020). "Progress of the applications of bio-oil," *Renew. Sustain. Energy Rev.* 134, article ID 110124. DOI: 10.1016/j.rser.2020.110124

Hu, X., Guo, H., Gholizadeh, M., Sattari, B., and Liu, Q. (2019). "Pyrolysis of different wood species: Impacts of C/H ratio in feedstock on distribution of pyrolysis products," *Biomass. Bioenerg.* 120, 28-39. DOI: 10.1016/j.biombioe.2018.10.021

Jahirul, M. I., Rasul, M. G., Chowdhury, A. A., and Ashwath, N. (2012). "Biofuels production through biomass pyrolysis – A technological review," *Energies* 5(12), 4952-5001. DOI: 10.3390/en5124952

Jayaseelan, A., Panchamoorthy G. K., SundarRajan, P., Rajagopal, M., and Pattabhiraman, A. (2020). "Hydrothermal liquefaction and pyrolysis of *Amphiroa fragilissima* biomass: Comparative study on oxygen content and storage stability parameters," *Bioresour. Technol. Rep.* 11, article ID 100465. DOI:

10.1016/j.biteb.2020.100465
Jena, U., and Das, K. C. (2011). "Comparative evaluation of thermochemical liquefaction and pyrolysis for bio-oil production from microalgae," *Energ. Fuel.* 25, 5472-5482. DOI: 10.1021/ef201373m
Jo, H., Verma, D., and Kim, J. (2018). "Excellent aging stability of upgraded fast pyrolysis bio-oil in supercritical ethanol," *Fuel* 232, 610-619. DOI: 10.1016/j.fuel.2018.06.005
Li, Q., Steele, P. H., Yu, F., Mitchell, B., and Hassan, E. B. (2013). "Pyrolytic spray increases levoglucosan production during fast pyrolysis," *J. Anal. Appl. Pyrolysis* 100, 33-40. DOI: 10.1016/j.jaap.2012.11.013
Liu, Y., Yuan, X., Huang, H., Wang, X., Wang, H., and Zeng, G. (2013). "Thermochemical liquefaction of rice husk for bio-oil production in mixed solvent (ethanol-water)," *Fuel Process. Technol.* 112, 93-99. DOI: 10.1016/j.fuproc.2013.03.005
Mahadevan, R., Shakya, R., Neupane, S., and Adhikari, S. (2015). "Physical and chemical properties and accelerated aging test of bio-oil produced from *in situ* catalytic pyrolysis in a bench-scale fluidized-bed reactor," *Energ. Fuel.* 29(2), 841-848. DOI: 10.1021/ef502353m
Mathanker, A., Pudasainee, D., Kumar, A., and Gupta, R. (2020). "Hydrothermal liquefaction of lignocellulosic biomass feedstock to produce biofuels: Parametric study and products characterization," *Fuel* 271, article ID 117534. DOI: 10.1016/j.fuel.2020.117534
Nazari, L., Yuan, Z., Souzanchi, S., Ray, M. B., and Xu, C. (2015). "Hydrothermal liquefaction of woody biomass in hot-compressed water: Catalyst screening and comprehensive characterization of bio-crude oils," *Fuel* 162, 74-83. DOI: 10.1016/j.fuel.2015.08.055
Ni, M., Leung, D. Y. C., Leung, M. K. H., and Sumathy, K. (2006). "An overview of hydrogen production from biomass," *Fuel Process. Technol.* 87(5), 461-472. DOI: 10.1016/j.fuproc.2005.11.003
Perlack, R. D., Wright, L. L., Turhollow, A., Graham, R. L., Stokes, B., and Erbach, D. C. (2005). *Biomass as Feedstock for a Bioenergy and Bioproducts Industry: The Technical Feasibility of a Billion-Ton Annual Supply* (Report No. DOE/GO-102005-2135; ORNL/TM-2005/66), Oak Ridge National Laboratory, Oak Ridge, TN, USA.
Peterson, A. A., Vogel, F., Lachance, R. P., Fröling, M., Antal, M. J., and Tester, J. W. (2008). "Thermochemical biofuel production in hydrothermal media: A review of sub- and supercritical water technologies," *Energy Environ. Sci.* 1, 32-65. DOI: 10.1039/b810100k
Pu, Y., Cao, S., and Ragauskas, A. J. (2011). "Application of quantitative ^{31}P NMR in biomass lignin and biofuel precursors characterization," *Energy Environ. Sci.* 4(9), 3154-3166. DOI: 10.1039/c1ee01201k
Qian, Y., Zuo, C., Tan, J., and He, J. (2007). "Structural analysis of bio-oils from sub-and supercritical water liquefaction of woody biomass," *Energy* 32(3), 196-202. DOI: 10.1016/j.energy.2006.03.027
Qu, T., Guo, W., Shen, L., Xiao, J., and Zhao, K. (2011). "Experimental study of biomass pyrolysis based on three major components: Hemicellulose, cellulose, and lignin," *Ind. Eng. Chem. Res.* 50(18), 10424-10433. DOI: 10.1021/ie1025453
Sasaki, C., Wanaka, M., Takagi, H., Tamura, S., Asada, C., and Nakamura, Y. (2013). "Evaluation of epoxy resins synthesized from steam-exploded bamboo lignin," *Ind.*

Crop. Prod. 43, 757-761. DOI: 10.1016/j.indcrop.2012.08.018

Singh, R., Prakash, A., Balagurumurthy, B., Singh, R., Saran, S., and Bhaskar, T. (2015). "Hydrothermal liquefaction of agricultural and forest biomass residue: Comparative study," *J. Mater. Cycles Waste.* 17, 442-452. DOI: 10.1007/s10163-014-0277-3

Street, J., Yu, F., Yan, Q., Wooten, J., Columbus, E., and Hassan, E. B. (2016). "Pilot-plant production of gas-to-liquid synthetic fuel using gasified biomass over a novel biochar-supported catalyst," *T. ASAE* 59(6), 1485-1496. DOI: 10.13031/trans.59.11887

Sun, P., Heng, M., Sun, S., and Chen, J. (2010). "Direct liquefaction of paulownia in hot compressed water: Influence of catalysts," *Energy* 35(12), 5421-5429. DOI: 10.1016/j.energy.2010.07.005

Tekin, K., Karagöz, S., and Bektaş, S. (2014). "A review of hydrothermal biomass processing," *Renew. Sustain. Energy Rev.* 40, 673-687. DOI: 10.1016/j.rser.2014.07.216

Thangalazhy-Gopakumar, S., Adhikari, S., Ravindran, H., Gupta, R. B., Fasina, O., Tu, M., and Fernando, S. D. (2010). "Physiochemical properties of bio-oil produced at various temperatures from pine wood using an auger reactor," *Bioresour. Technol.* 101(21), 8389-8395. DOI: 10.1016/j.biortech.2010.05.040

Vardon, D. R., Sharma, B. K., Blazina, G. V., Rajagopalan, K., and Strathmann, T. J. (2012). "Thermochemical conversion of raw and defatted algal biomass *via* hydrothermal liquefaction and slow pyrolysis," *Bioresour. Technol.* 109, 178-187. DOI: 10.1016/j.biortech.2012.01.008

Xu, C., Arancon, R. A. D., Labidi, J., and Luque, R. (2014). "Lignin depolymerisation strategies: Towards valuable chemicals and fuels," *Chem. Soc. Rev.* 43(22), 7485-7500. DOI: 10.1039/c4cs00235k

Yuan, X. Z., Li, H., Zeng, G. M., Tong, J. Y., and Xie, W. (2007). "Sub- and supercritical liquefaction of rice straw in the presence of ethanol-water and 2-propanol-water mixture," *Energy* 32(11), 2081-2088. DOI: 10.1016/j.energy.2007.04.011

Zhang, W., Henschel, T., Söderlind, U., Tran, K., and Han, X. (2017). "Thermogravimetric and online gas analysis on various biomass fuels," *Energy Procedia* 105, 162-167. DOI: 10.1016/j.egypro.2017.03.296

Article submitted: September 16, 2021; Peer review completed: October 30, 2021; Revised version received and accepted: December 16, 2021; Published: February 18, 2022.
DOI: 10.15376/biores.17.2.2176-2192

APPENDIX

Supplemental Material

Table S1. OH numbers of HTL and FP bio-oils calculated by quantitative ^{31}P NMR after derivatization with TMDP

OH Type	HTL (mmol/g)	Pyrolysis (mmol/g)	Integration Region (ppm)
Aliphatic	5.01 ± 0.09	5.61 ± 0.03	150.0 – 145.5
Phenolic	3.21 ± 0.1	3.22 ± 0.1	144.7 – 137.3
B-5	*0.16 ± 0.0*	*0.26 ± 0.01*	144.7 – 142.8
4-O-5	*0.27 ± 0.01*	*0.30 ± 0.02*	142.8 – 141.7
5-5	*0.60 ± 0.02*	*0.69 ± 0.08*	141.7 – 140.2
Guaiacyl	*1.43 ± 0.09*	*1.04 ± 0.01*	140.2 – 139.0
Catechol	*0.47 ± 0.01*	*0.65 ± 0.0*	139.0 – 138.2
p-OH	*0.27 ± 0.02*	*0.26 ± 0.0*	138.2 – 137.3
Acidic	1.04 ± 0.09	*1.47 ± 0.11*	136.6 – 133.6
Total	**9.25 ± 0.09**	**10.30 ± 0.02**	